

STUDY OF
XENON INDUCED POWER OSCILLATIONS
WITH λ -MODES

By

Ioannis A. Anastasiou

PART A: ON-CAMPUS PROJECT

A project report submitted in partial fulfillment of
the requirements for the degree of
Master of Engineering

Department of Engineering Physics
McMaster University
Hamilton, Ontario

MASTER OF ENGINEERING
(Engineering Physics)

McMASTER UNIVERSITY
Hamilton, Ontario

TITLE (PART A): Study of Xenon Induced Power Oscillations with
 λ -Modes.

AUTHOR: Ioannis A. Anastasiou

SUPERVISOR: Dr. O. A. Trojan

NUMBER OF PAGES: vii, 42.

ABSTRACT

A large thermal reactor operating at sufficiently high flux levels is susceptible to oscillations in the power distribution that are associated with a periodic redistribution of xenon poison.

The particular perturbation method, λ -mode approximation, is presented in this report. A detailed description of the λ -mode mathematical formalism and the computer program XIPOLML and its application to Pickering reactors are reported.

ACKNOWLEDGMENTS

The author would like to express his thanks to Dr. O.A. Trojan for many discussions and suggestions and his continuous guidance.

Mr. Madat Mamourian's very substantial help in every step of this study is deeply appreciated.

TABLE OF CONTENTS

	<u>PAGE</u>
1. INTRODUCTION	1
2. MATHEMATICAL FORMALISM	2
3. ANALYSIS AND RESULTS	15
4. REFERENCES	18
APPENDICES	
1. XIP01ML User's Guide	31
2. XIP01ML Program Listing	36

LIST OF TABLES

1. Material properties at full power
2. Material properties at 50% of full power
3. Xenon parameters
4. Properties of reactivity devices
5. Subcriticality of first harmonic
6. Materials used for generation of the modes
7. Materials used in XIP01ML
8. Threshold power, period subcriticality and the values of the parameters Ω and η at 100% and 50% of full power

LIST OF FIGURES

1. Octant core model
2. Period, peak-to-peak ratio vs percent of full power, $\rho = -14.307$ mk
and $\rho = -14.039$ mk
3. Period, peak-to-peak ratio vs percent of full power, $\rho = -14.356$ mk
4. Percent power level vs the real part (P_r)
5. Period, peak-to-peak ratio vs percent of full power, $\rho = -16.24$ mk
6. Period, peak-to-peak ratio vs percent of full power, $\rho = -18.00$ mk

1. INTRODUCTION

Let us suppose that into a reactor operating at constant total power, for a sufficiently long time to have established an equilibrium xenon distribution, we introduce a flux tilt. Let us further suppose that the tilt is a side to side tilt, such that the average flux in the left half is increased and in the right half decreased to maintain constant total power. This tilt will cause the xenon to burn out more rapidly in the left half and less rapidly in the right half, while the local rates of formation of xenon from iodine decay remain nearly constant for some time. The reactivity increases then in the left half of the reactor and decreases in the right half. If no spatial flux control is imposed on top of bulk reactivity control the tilt will be amplified. Ultimately the growth of the xenon from the iodine that is forming more rapidly in the left half, and the decay of xenon together with lower production in the right half, reverse the reactivity distribution and the power will peak in the right half of the reactor. These oscillations may persist or grow unless spatial flux control is imposed.

Xenon induced oscillations can occur only at sufficiently high flux levels, at which rate of xenon burnout is important relative to the rate of xenon decay. Further, they can occur only in thermal reactors since the neutron energy spectrum, in a fast or intermediate reactor is such that the corresponding absorption cross section of xenon-135 is quite small. Furthermore, it is necessary for the reactor to have dimensions, which are large compared to neutron migration length, because only in such systems can the spatial harmonics of the flux be excited to an appreciable extent.

Xenon poisoning in reactors was discovered when the first production reactor operated at Hanford, and xenon instability was first observed when local hot spots were detected in the Hanford reactors. The first clear demonstration of flux-tilt oscillations was obtained at Savannah River and reported by Haefner⁽¹⁾. In December 1955 an undamped axial flux oscillation occurred and persisted for 14 days in a reactor held at constant power. The period of the oscillation was 28 hours. Only later was this identified as a xenon-induced oscillation.

For Pickering power reactors, instability of the first azimuthal mode was observed in Unit #1 in early June, 1971 while operating at full power. Although the source of the perturbation as well as when it occurred remain unknown, the side to side oscillation in the flux distribution grew steadily with a period of approximately twenty hours until control action was initiated to terminate the oscillation⁽²⁾.

In this report the technique of W.M. Stacey, Jr.⁽³⁾ is presented, and it is used in the computation of the threshold value for Pickering reactors. W.M. Stacey, Jr. makes use of possibly the most computationally tractable method appropriate for the analysis of realistic reactor models. He utilizes a spatial expansion in λ -modes, which are the eigenfunctions of the standard equation for the static neutron flux, with equilibrium xenon and temperature feedback effects implicit in the cross sections. This analysis proceeds by linearizing the appropriate neutron balance equations, Laplace transforming, and expanding the spatial dependence in eigenfunctions associated with the steady-state reactor model. This results in a transfer function type relation, and a stability criterion is derived from the requirement that the real part of the poles of the transfer function be negative, which ensures an exponentially decaying power oscillation.

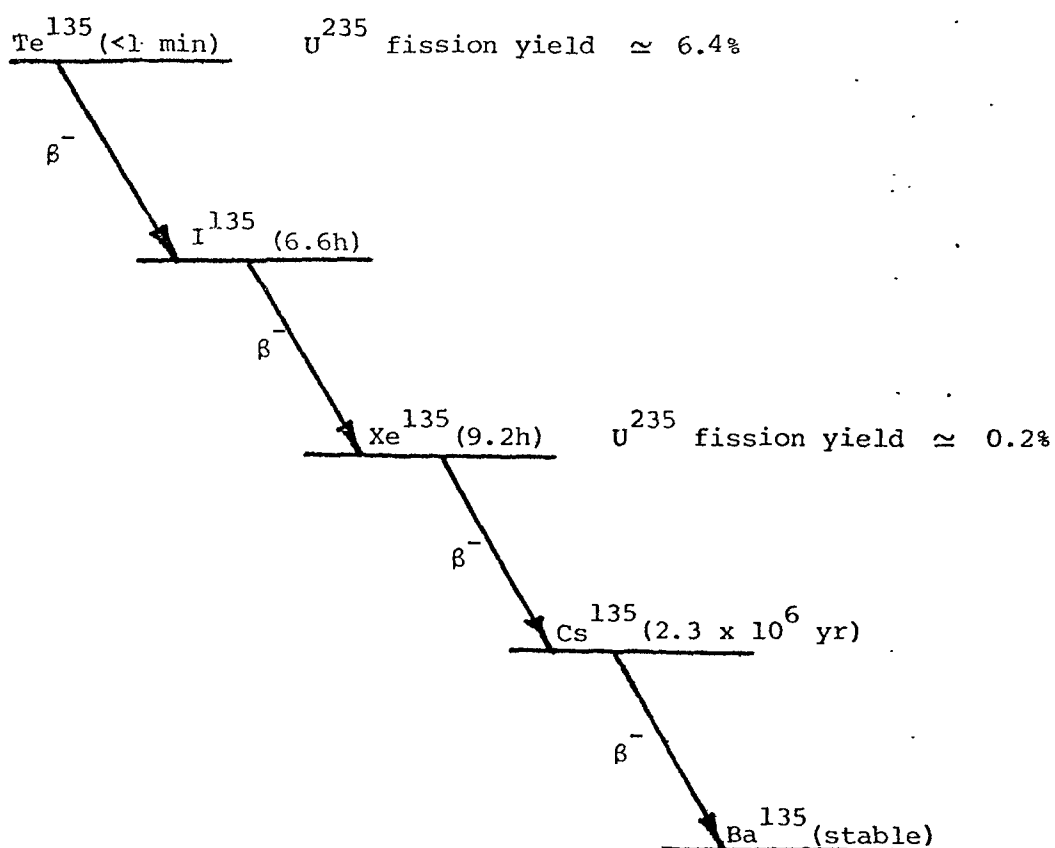
Although a linear analysis is inadequate when the magnitude of the power oscillation is comparable with the mean power level, it should be sufficient to predict the tendency of a small oscillation to grow or decay, i.e. yield a stability criterion. Furthermore, power oscillations of a few percent might be acceptable, and a linear analysis should describe these.

2. MATHEMATICAL FORMALISM

It is well known that the fission product xenon-135, with a half-life of 9.2 hours, has a very large absorption cross section for thermal neutrons, about 2.6×10^6 barns⁽⁴⁾. A small fraction of this nuclear species is formed directly in fission, but the major portion results from the decay of iodine-135, with a half-life of 6.6 hours. Iodine-135 is itself a decay product of

tellurium-135, which has a half-life of less than 1 minute. Consequently, for all practical purposes, it may be assumed that the production of xenon-135 is determined almost solely by the decay of iodine-135, and that the rate of formation of the latter is proportional to the fission rate.

The fission-product-decay chain is shown below.



A flux tilt, induced by a random reactivity perturbation, is at first enhanced by the tilted xenon burnup rate distribution and later compensated by the tilted xenon production rate. Under certain conditions the compensation is excessive, and diverging spatial power oscillations are induced.

Because of the time scale of the iodine and xenon dynamics, prompt and delayed neutron dynamics may be neglected, i.e. changes in the neutron flux are assumed to occur instantaneously, and the delayed neutron precursors are assumed to be always in equilibrium. Moreover, as mentioned earlier, iodine-135 can be assumed to be formed directly from fission. As xenon feedback is assumed to affect only the thermal neutron balance, the two-group neutron balance equations and the xenon and iodine equations, using the standard notation may be written as

$$D_1 \nabla^2 \phi_1(r, t) - \left\{ \Sigma_{a,1}(r) + \Sigma_R(r) \right\} \phi_1(r, t) + \frac{\nu}{k_0} \Sigma_{f,2}(r) \phi_2(r, t) = 0 \quad \dots (1)$$

$$D_2 \nabla^2 \phi_2(r, t) - \left\{ \Sigma_{a,2}(r) + \sigma_x X(r, t) \right\} \phi_2(r, t) + \Sigma_R(r) \phi_1(r, t) = 0 \quad \dots (2)$$

$$\gamma_I \Sigma_{f,2}(r) \phi_2(r, t) - \lambda_I I(r, t) = \frac{\delta I(r, t)}{\delta t} \quad \dots (3)$$

$$\gamma_X \Sigma_{f,2}(r) \phi_2(r, t) + \lambda_I I(r, t) - \lambda_X X(r, t) - \sigma_X X(r, t) \phi_2(r, t) = \frac{\delta X(r, t)}{\delta t} \quad \dots (4)$$

The eigenfunctions, λ -modes, satisfy the equilibrium neutron balance equations, which in matrix form are

$$\left\{ \begin{array}{l} \left[\begin{array}{cc} -D_1 \nabla^2 + \{ \Sigma_{a,1}(r) + \Sigma_R(r) \} & 0 \\ -\Sigma_R(r) & -D_2 \nabla^2 + \{ \Sigma_{a,2}(r) + \sigma_x X_0(r) \} \end{array} \right] \\ - \frac{1}{k_n} \left[\begin{array}{cc} 0 & v \Sigma_{f,2}(r) \\ 0 & 0 \end{array} \right] \end{array} \right\} \begin{bmatrix} \psi_{n,1}(r) \\ \psi_{n,2}(r) \end{bmatrix} = 0 \quad \dots (5)$$

$$\text{or } (\bar{L} - \frac{1}{k_n} \bar{M}) \cdot \bar{\psi}_n = 0 \quad \dots (6)$$

where \bar{L} and \bar{M} may be regarded as the destruction and production matrices respectively.

The adjoint eigenfunctions $\psi_{n,1}^*(r)$, $\psi_{n,2}^*(r)$ satisfy the adjoint equation of (6).

$$(\bar{L}^* - \frac{1}{k_n} \bar{M}^*) \cdot \bar{\psi}_n^* = 0 \quad \dots (7)$$

where

$$L^{-*} = \begin{bmatrix} -D_1 \nabla^2 + \left\{ \Sigma_{a,1}(r) + \Sigma_R(r) \right\} & -\Sigma_R(r) \\ 0 & -D_2 \nabla^2 + \left\{ \Sigma_{a,2}(r) + \sigma_x X_o(r) \right\} \end{bmatrix}$$

and

$$M^{-*} = \begin{bmatrix} 0 & 0 \\ v \Sigma_{f,2}(r) & 0 \end{bmatrix}$$

The λ -modes are biorthogonal with respect to the production matrix M , and may be normalized such that:

$$\int \psi_{m,1}^*(r) v \Sigma_{f,2}(r) \psi_{n,2}(r) dV = \delta_{m,n} \quad (8)$$

An equivalent normalization condition can be obtained, taking the neutron balance of fast flux and its adjoint, after premultiplying the former with $\psi_{n,1}^*(r)$ and the latter with $\psi_{n,1}(r)$ and integrating over the volume:

$$\begin{aligned} \int \psi_{n,1}^*(r) D_1 \nabla^2 \psi_{n,1}(r) dV - \int \psi_{n,1}^*(r) (\Sigma_{a,1}(r) + \Sigma_R(r)) \psi_{n,1}(r) dV + \\ + \int \frac{1}{k_n} \psi_{n,1}^*(r) v \Sigma_{f,2}(r) \psi_{n,2}(r) dV = 0 \end{aligned} \quad (9)$$

$$\begin{aligned} \int \psi_{n,1}(r) D_1 \nabla^2 \psi_{n,1}^*(r) dV - \int \psi_{n,1}(r) \left((\Sigma_{a,1}(r) + \Sigma_R(r)) \psi_{n,1}^*(r) \right) dV + \\ + \int \psi_{n,1}(r) \Sigma_R(r) \psi_{n,2}^*(r) dV = 0 \end{aligned} \quad (10)$$

Subtracting (10) from (9), we have

$$\int \psi_{n,1}^*(r) v \Sigma_{f,2}(r) \psi_{n,2}(r) dV = k_n \int \psi_{n,2}^*(r) \Sigma_R(r) \psi_{n,1}(r) dV \quad (11)$$

From this equation (11) and the normalization condition (8), it can be seen that an equivalent normalization condition is:

$$k_n \int \psi_{m,2}^*(r) \Sigma_R(r) \psi_{n,1}(r) dV = \delta_{m,n} \quad (12)$$

The solution of Equations (1) to (4) by analytical methods is difficult because of the non-linearity introduced by the xenon absorption term. Implicit non-linearities are also introduced by the dependence of the cross sections of the flux via the temperature feedback.

Linearizing these equations reduces their complexity, but also reduces their applicability to a small region about the equilibrium point. The linearized equations are used principally for investigations of stability.

The linearized equations are obtained by expanding about the equilibrium point, denoted by a zero subscript:

$$\phi_1(r,t) = \phi_{o,1}(r) + \delta\phi_1(r,t) \quad \dots (13)$$

$$\phi_2(r,t) = \phi_{o,2}(r) + \delta\phi_2(r,t) \quad \dots (14)$$

$$I(r,t) = I_o(r) + \delta I(r,t) \quad \dots (15)$$

$$X(r,t) = X_o(r) + \delta X(r,t) \quad \dots (16)$$

The effect of temperature feedback should be taken into account at this stage:

The fission cross section may be flux-dependent:

$$\Sigma_{f,2}(\phi_2) = \Sigma_{f,2}(\phi_{o,2}) [1 + (\phi_2 - \phi_{o,2})\alpha] \quad \dots (17)$$

where α is the power coefficient and $\phi_{o,2}$ is a reference flux distribution. This reference flux distribution may have a single value throughout the core.

Both sides of Equation (17) are multiplied by $\phi_2 (= \phi_{o,2} + \delta\phi_2)$ to get:

$$\begin{aligned} \Sigma_{f,2}(\phi_2)\phi_2 &= \Sigma_{f,2}(\phi_{o,2}) \left[1 + (\phi_2 - \phi_{o,2}) \alpha \right] \left[\phi_{o,2} + \delta\phi_2 \right] \\ &= \underbrace{\Sigma_{f,2}(\phi_{o,2})\phi_{o,2}}_A + \underbrace{\Sigma_{f,2}(\phi_{o,2})\delta\phi_2}_{B} + \underbrace{\alpha \Sigma_{f,2}(\phi_{o,2})\phi_{o,2}\delta\phi_2}_{C} + \underbrace{\Sigma_{f,2}(\phi_{o,2})(\delta\phi_2)^2}_D \end{aligned} \quad (18)$$

- where
- A steady-state term,
 - B the effect of the perturbation $\delta\phi_2$ without feedback,
 - C the temperature feedback term, and
 - D can be neglected as being very small.

The linearized equations (13) to (16) are imposed on equations (1) to (4). Use is made of the fact that the steady-state solutions satisfy the time-independent version of equations (1) to (4). The terms that are non-linear in $\delta\phi_1$, $\delta\phi_2$, and δX are neglected. The temperature feedback term (C) is added to the thermal neutron balance equation, according to equation (18). The four equation system (1) to (4) finally becomes

$$D_1 \nabla^2 \delta\phi_1(r,t) - \{ \Sigma_{a,1}(r) + \Sigma_R(r) \} \delta\phi_1(r,t) + \frac{\nu}{k_0} \Sigma_{f,2}(r) \delta\phi_2(r,t) = 0 \quad (19)$$

$$\begin{aligned} \Sigma_R(r) \delta\phi_1(r,t) + D_2 \nabla^2 \delta\phi_2(r,t) - \{ \Sigma_{a,2}(r) + \sigma_x X_0(r) \} \delta\phi_2(r,t) - \\ - \sigma_x \phi_{o,2}(r) \delta X(r,t) + \alpha \Sigma_{f,2}(r) \phi_{o,2}(r) \delta\phi_2(r,t) = 0 \end{aligned} \quad (20)$$

$$\gamma_I \Sigma_{f,2}(r) \delta \phi_2(r,t) - \lambda_I \delta I(r,t) = \frac{\partial \delta I(r,t)}{\partial t} \quad (21)$$

$$\begin{aligned} \gamma_x \Sigma_{f,2}(r) \delta \phi_2(r,t) - \sigma_x X_o(r) \delta \phi_2(r,t) - \lambda_x \delta X(r,t) - \sigma_x \phi_{o,2}(r) \delta X(r,t) + \\ + \lambda_I \delta I(r,t) = \frac{\partial \delta X(r,t)}{\partial t} \end{aligned} \quad (22)$$

Equations (19) to (22) are Laplace transformed according to:

$$L \left\{ f(r,t) \right\} = \int_0^{\infty} e^{-pt} f(r,t) dt = F(r,p) \quad (23)$$

$$L \left\{ \dot{f}(r,t) \right\} = pF(r,p) - f(r,t=0) \quad (24)$$

where f stands for ϕ_1 , ϕ_2 , X and I , and the dot denotes the first derivative with respect to time. At this stage, the iodine concentration term $\delta I(r,p)$ is eliminated between equations (21) and (22), and a three-equation system is obtained:

$$\left(-D_1 \nabla^2 + \Sigma_{a,1}(r) + \Sigma_R(r) \right) \delta \phi_1(r,p) - \left(\frac{v}{k_o} \Sigma_{f,2}(r) \right) \delta \phi_2(r,p) = 0 \quad (25)$$

$$\begin{aligned} \left(-\Sigma_R(r) \right) \delta \phi_1(r,p) + \left(-D_2 \nabla^2 + \Sigma_{a,2}(r) + \sigma_x X_o(r) - \alpha \Sigma_{f,2}(r) \phi_{o,2}(r) \right) \delta \phi_2(r,p) + \\ + \sigma_x \phi_{o,2}(r) \delta X(r,p) = 0 \end{aligned} \quad (26)$$

$$\begin{aligned} \left(p + \lambda_x + \sigma_x \phi_{o,2}(r) \right) \delta X(r,p) = \left[\gamma_x \Sigma_{f,2}(r) + \left(\frac{\lambda_I}{p + \lambda_I} \right) \gamma_I \Sigma_{f,2}(r) - \sigma_x X_o(r) \right] \delta \phi_2(r,p) + \\ + \left[\left(\frac{\lambda_I}{p + \lambda_I} \right) \delta I(r,t=0) + \delta X(r,t=0) \right] \end{aligned} \quad (27)$$

Expansion in λ -Modes

The flux and xenon perturbations are expanded in λ -modes as defined by equation (5).

$$\delta\phi_1(r,p) = \sum_{n=1}^N D_n(p) \psi_{n,1}(r) \quad \dots (28)$$

$$\delta\phi_2(r,p) = \sum_{n=1}^N A_n(p) \psi_{n,2}(r) \quad \dots (29)$$

$$\delta X(r,p) = \sum_{n=1}^N B_n(p) \Sigma_{f,2}(r) \psi_{n,2}(r) \quad \dots (30)$$

If it is assumed that the first harmonic is adequate to represent the variations in the flux and xenon from the equilibrium distributions, thus only the first term is retained in the expansions of equations (28) to (30):

$$\delta\phi_1(r,p) \approx D_1(p) \psi_{1,1}(r) \quad \dots (31)$$

$$\delta\phi_2(r,p) \approx A_1(p) \psi_{1,2}(r) \quad \dots (32)$$

$$\delta X(r,p) \approx B_1(p) \Sigma_{f,2}(r) \psi_{1,2}(r) \quad \dots (33)$$

For simplicity the subscript "1" referring to the mode is omitted. Using the expansion of equations (31) to (33), the three-equation system (25) to (27) becomes:

$$\left(-D_1 \nabla^2 + \Sigma_{a,1}(r) + \Sigma_R(r)\right) D(p) \psi_1(r) = \left(\frac{v}{k_0} \Sigma_{f,2}(r)\right) A(p) \psi_2(r) \quad \dots (34)$$

$$\begin{aligned} \left(-\Sigma_R(r)\right) D(p) \psi_1(r) + \left(-D_2 \nabla^2 + \Sigma_{a,2}(r) + \sigma_x X_0(r) - \alpha \Sigma_{f,2}(r) \emptyset_{0,2}(r)\right) A(p) \psi_2(r) + \\ + \sigma_x \emptyset_{0,2}(r) \Sigma_{f,2}(r) B(p) \psi_2(r) = 0 \quad \dots (35) \end{aligned}$$

$$\begin{aligned} \left(p + \lambda_x + \sigma_x \emptyset_{0,2}(r)\right) \Sigma_{f,2}(r) B(p) \psi_2(r) = \left(\gamma_x \Sigma_{f,2}(r) + \frac{\lambda_I}{p + \lambda_I} \gamma_I \Sigma_{f,2}(r) - \right. \\ \left. - \sigma_x X_0(r)\right) A(p) \psi_2(r) + \left(\frac{\lambda_I}{p + \lambda_I} \delta I(r, t = 0) + \delta X(r, t = 0)\right) \quad \dots (36) \end{aligned}$$

Using the definition of λ -eigenfunctions, the L.H.S. of equation (34) can be written as:

$$\left(-D_1 \nabla^2 + \Sigma_{a,1}(r) + \Sigma_R(r)\right) D(p) \psi_1(r) = \frac{v}{k_1} \Sigma_{f,2}(r) D(p) \psi_2(r) \quad \dots (37)$$

$$\text{i.e. } \frac{v}{k_1} \Sigma_{f,2}(r) D(p) \psi_2(r) = \frac{v}{k_0} \Sigma_{f,2}(r) A(p) \psi_2(r) \quad \dots (38)$$

$$\text{or } D(p) = \frac{k_1}{k_0} A(p) \quad \dots (39)$$

Using equation (39) and the definition of λ -eigenfunctions, equation (35) becomes

$$A(p) \left(1 - \frac{k_1}{k_0} \right) \Sigma_R(r) \psi_1(r) - A(p) \alpha \Sigma_{f,2}(r) \varnothing_{0,2}(r) \psi_2(r) + \\ + B(p) \sigma_x \Sigma_{f,2}(r) \varnothing_{0,2}(r) \psi_2(r) = 0 \quad (40)$$

Multiplying every term of equation (40) by $\psi_2^*(r)$, integrating over the whole core and employing the normalization condition (12), the following expression is obtained, after dividing each term by $\int \psi_2^*(r) \Sigma_{f,2}(r) \psi_2(r) dV$:

$$A(p) \left\{ \frac{\frac{1}{k_1} - \frac{1}{k_0}}{\int \psi_2^*(r) \Sigma_{f,2}(r) \psi_2(r) dV} - \frac{\int \psi_2^*(r) \alpha \Sigma_{f,2}(r) \varnothing_{0,2}(r) \psi_2(r) dV}{\int \psi_2^*(r) \Sigma_{f,2}(r) \psi_2(r) dV} \right\} + \\ + B(p) \left\{ \frac{\int \psi_2^*(r) \sigma_x \Sigma_{f,2}(r) \varnothing_{0,2}(r) \psi_2(r) dV}{\int \psi_2^*(r) \Sigma_{f,2}(r) \psi_2(r) dV} \right\} = 0 \quad (41)$$

$$\text{or} \quad B(p) = - \frac{\Omega}{\lambda_x \eta} A(p) \quad (42)$$

$$\text{where} \quad \Omega = \frac{\frac{1}{k_1} - \frac{1}{k_0}}{\int \psi_2^*(r) \Sigma_{f,2}(r) \psi_2(r) dV} - \frac{\int \psi_2^*(r) \alpha \Sigma_{f,2}(r) \varnothing_{0,2}(r) \psi_2(r) dV}{\int \psi_2^*(r) \Sigma_{f,2}(r) \psi_2(r) dV} \quad (43)$$

$$\eta = \frac{1}{\lambda_x} \frac{\int \psi_2^*(r) \sigma_x \Sigma_{f,2}(r) \varnothing_{0,2}(r) \psi_2(r) dV}{\int \psi_2^*(r) \Sigma_{f,2}(r) \psi_2(r) dV} \quad (44)$$

Finally, the xenon equation, (36), after multiplying each term by $\psi_2^*(r)$ and integrating over the whole volume, becomes:

$$\begin{aligned}
& - (p + \lambda_x) \frac{A(p)\Omega}{\lambda_x \eta} \int \psi_2^*(r) \Sigma_{f,2}(r) \psi_2(r) dV - \\
& \quad - \frac{A(p)\Omega}{\lambda_x \eta} \int \psi_2^*(r) \sigma_x \Sigma_{f,2}(r) \vartheta_{o,2}(r) \psi_2(r) dV = \\
& = \left(\gamma_x + \frac{\lambda_I \gamma_I}{p + \lambda_I} \right) A(p) \int \psi_2^*(r) \Sigma_{f,2}(r) \psi_2(r) dV - A(p) \int \psi_2^*(r) \sigma_x X_o(r) \psi_2(r) dV + R^1
\end{aligned} \tag{45}$$

where $R^1 = \int S \psi_2^*(r) dV$

and $S = \frac{\lambda_I}{p + \lambda_I} \delta I(r, t = 0) + \delta X(r, t = 0)$ is the inhomogeneous term involving initial values of δX and δI .

Dividing each term by $\sigma_x \int \psi_2^*(r) \Sigma_{f,2}(r) \vartheta_{o,2}(r) \psi_2(r) dV$ and putting:

$$\frac{1 + \beta}{\gamma_I + \gamma_x} = \frac{\int \psi_2^*(r) \Sigma_{f,2}(r) \vartheta_{o,2}(r) \psi_2(r) dV}{\int \psi_2^*(r) \lambda_x X_o(r) \psi_2(r) dV}$$

the following equation is obtained:

$$\frac{A(p)}{\lambda_x \eta} \left(\gamma_x + \frac{\lambda_I \gamma_I}{p + \lambda_I} - \eta \frac{\gamma_I + \gamma_x}{1 + \beta} + \Omega + \frac{p + \lambda_x}{\lambda_x \eta} \right) = \frac{-R^1}{\sigma_x \int \psi_2^*(r) \Sigma_{f,2}(r) \vartheta_{o,2}(r) \psi_2(r) dV} = F
\end{aligned} \tag{46}$$

or $A(p) = H(p) \lambda_x \eta R$ (47)

where $H(p) = \frac{1}{\gamma_x + \frac{\lambda_I \gamma_I}{p + \lambda_I} - \eta \frac{\gamma_I + \gamma_x}{1 + \beta} + \Omega + \frac{p + \lambda_x}{\lambda_x \eta}} = \frac{Z (p + \lambda_I)}{(P - P_1) (P - P_2)}$ (48)

Z: Constant with respect to p

is the transfer function relating the coefficient $A(p)$ with the inhomogeneous term R .

The poles of the transfer function H can be found from Equation (48) which after some algebra becomes:

$$P_1 = -P_r + i(C - P_r^2)^{1/2}$$

$$P_2 = -P_r - i(C - P_r^2)^{1/2}$$

where

$$P_r = \frac{\lambda_x}{2} \left\{ \left(1 + \frac{\lambda_I}{\lambda_x} + \eta \right) - \frac{\eta}{\Omega} \left(\frac{\gamma_I + \gamma_x}{1 + \beta} \eta - \gamma_x \right) \right\} \quad (49)$$

$$C = \lambda_I \lambda_x \left\{ (1 + \eta) + \eta \frac{(\gamma_I + \gamma_x)}{\Omega} \left(1 - \frac{\eta}{1 + \beta} \right) \right\} \quad (50)$$

and the condition of stability is that

$$P_r > 0 \quad (51)$$

i.e. the poles of the transfer function lie in the left half complex p-plane and the period of oscillation is calculated from:

$$T = \frac{2\pi}{(C - P_r^2)^{1/2}} \quad (52)$$

It is clear from the condition of stability ($P_r > 0$), that it is mostly controlled by the physical parameters Ω and η . The quantity Ω defined by equation (43) is primarily decided by the subcriticality of the perturbation mode under study, and it is obvious that a reactor becomes less stable when reactor harmonics become more easily excitable, i.e. when the amount of subcriticality of a mode decreases. This occurs when the dimensions of the core are increased or when the power distribution is flattened. A negative power coefficient ($\alpha < 0$) increases Ω , thus making a reactor more stable. As for the quantity η defined by equation (44), it is seen, that η is proportional to the thermal flux level, i.e. power level and an increase in it is generally destabilizing.

3. ANALYSIS AND RESULTS

In order to test the previous mathematical analysis, the stability of the Pickering initial core to xenon induced power oscillations in the side-to-side mode was analyzed using XIPOLML*, a program specifically created for this purpose. The flux and xenon distributions at steady state, the first azimuthal harmonic and its adjoint were generated with the SORGHUM(5) code. Feedback reactivity effects at various power levels were included in the analysis.

The measure of stability of spatial oscillations in XIPOLML is the peak-to-peak ratio

$$R = \exp(-P_r T)$$

i.e. the ratio between maximum (or minimum) values of tilt $\left(\frac{P_L - P_R}{P_L + P_R}\right)$ during successive cycles of the oscillations where:

- T : period of oscillation
- P_r : damping factor
- P_L and P_R : neutron production rates in the left and right halves of the reactor respectively.

These power oscillations will be unstable if the peak-to-peak ratio (R) is greater than 1, and will be damped if less than 1. At threshold, the peak-to-peak ratio is equal to 1.

* See Appendices

Analysis

Steady state conditions of the initial core, were calculated using a coarse mesh 57.15 cm x 57.15 cm x 16.719 cm octant core model (Fig. 1). The three adjuster rows of six rods each were located as follows: the central row in the transverse mid-plane and the outer rows 91.95 cm on either side of it. The material properties used in the study together with the $\Delta\Sigma_{a,2}$ for adjuster rods and zone controllers are given in Tables I-IV and VI, VII.

The following steady state distributions were generated:

- (a) distributions corresponding to 100% full power (1744 MW_f) with zone controllers almost empty;
- (b) distributions corresponding to 50% full power with zone controllers almost empty; and
- (c) distributions corresponding to 100% full power with zone controllers 35.5% full.

Next, the side-to-side mode and its adjoint were generated with SORGHUM. Mode subcriticality for each of the above cases are given in Table V.

Having generated the fundamental, the side-to-side and adjoint mode distributions, they were input into XIP01ML.

To examine the stability of the core at different power levels, the input steady state distributions and the power coefficients were reduced linearly and the xenon distributions according to the formula governing the equilibrium xenon concentration.

The behavior of peak-to-peak ratio and the period vs. percentage of full power for the different cases are given in Figures 2 and 3. From these figures the reactor power thresholds and the corresponding periods were obtained and they are listed in Table together with the corresponding values of the parameters

Next the study of spatial stability was extended to hypothetical reactor operating levels up to 400% of full power, and the reactor was found to tend to stabilize as the reactor power was raised above 200%. This is due to the existence of large negative power coefficients at high power levels (Figure 4).

A further step was undertaken⁽⁶⁾, to investigate the effect of the side-to-side mode subcriticality on the threshold. Using a value of 16.24 mk subcriticality found with the MONIC program, when calculating the flux harmonics, the threshold was found to be at 52% of full power (Figure 5). Finally, the subcriticality was changed to 18 mk based on first azimuthal mode reactivity measurements of Pickering⁺ and the threshold was found to be about 74% of full power (Figure 6). Note that in both of these cases where the subcriticality of the side-to-side mode was 14.307 mk.

In conclusion, it can be stated that this approach is quite a powerful tool in estimating the effect of various parameters on xenon stability.

+ Memorandum to A. A. Pasanen from A. P. Dastur, 44-06000, June 71.

4. REFERENCES

- (1) R.R. Haefner, "Flux Oscillations caused by Xenon Instability"; Nucl. Science Tech., 2 (3):291, Dec. 1956.
- (2) O.A. Trojan, private communication.
- (3) W.M. Stacey, Jr., "Linear Analysis of Xenon Spatial Oscillations", Nucl. Science Eng., 30, 453 (1967).
- (4) N.E. Holden and F.W. Walker, Chart of Nuclides, KAPL 11th edition, April 1972.
- (5) O.A. Trojan, " SORGHUM", TDAI-88, to be published.
- (6) M. Mamourian, private communication.

TABLES

TABLE I (*)

Material Properties at Full Power

Material	$\Sigma_{a,1}, \text{cm}^{-1}$	$\Sigma_{a,2}, \text{cm}^{-1}$	$\nu\Sigma_{f,2}, \text{cm}^{-1}$	Σ_R, cm^{-1}	Reactivity Change From 100% to Hot Shutdown (mk), α_f
Artificial	10^{10}	10^{10}	0	0	0
Reflector	10^{-11}	1.99821×10^{-4}	0	1.01811×10^{-2}	0
Fresh Fuel	7.86413×10^{-4}	3.88496×10^{-3}	4.64689×10^{-3}	7.36792×10^{-3}	-7.0×10^{-3}

TABLE II (**)

Material Properties at 50% of Full Power

Material	$\Sigma_{a,1}, \text{cm}^{-1}$	$\Sigma_{a,2}, \text{cm}^{-1}$	$\nu\Sigma_{f,2}, \text{cm}^{-1}$	Σ_R, cm^{-1}	Reactivity Change From 50% to Hot Shutdown (mk), α_f
Artificial	10^{10}	10^{10}	0	0	0
Reflector	10^{-11}	2.09379×10^{-4}	0	1.01811×10^{-2}	0
Fresh Fuel	7.69735×10^{-4}	3.92505×10^{-3}	4.69337×10^{-3}	7.39244×10^{-3}	-4.04×10^{-3}

* PPV-PKPBS-4

** PPV-PKPBS-6

TABLE IIIXenon Parameters

$$\begin{aligned}
 \lambda_I &= 2.94 \times 10^{-5} \text{ sec}^{-1} \\
 \lambda_X &= 2.10 \times 10^{-5} \text{ sec}^{-1} \\
 \gamma_I &= 6.44 \times 10^{-2} \\
 \gamma_X &= 2.30 \times 10^{-3} \\
 \sigma_X &= 1.219 \times 10^{-18} \text{ cm}^2 \\
 \nu &= 2.43 \text{ neutrons/fission}
 \end{aligned}$$

TABLE IV (*)Properties of Reactivity Devices

$$\begin{aligned}
 \Delta\Sigma_{a,2} \text{ (central row)} &= 0.54468 \times 10^{-3} \text{ cm}^{-1} \\
 \Delta\Sigma_{a,2} \text{ (outer row)} &= 1.15776 \times 10^{-3} \text{ cm}^{-1} \\
 \Delta\Sigma_{a,2} \text{ (zone controllers)} &= 11.74280 \times 10^{-4} \text{ cm}^{-1} \\
 \rho_{\text{ADJ}} \text{ (adjuster worth)} &= 18.502 \text{ mk (zone controllers almost empty)}
 \end{aligned}$$

TABLE VSubcriticality of First HarmonicZone Controllers almost empty

$$\begin{aligned}
 k_0 &= 1.0 \\
 k_1 &= 0.985894 \text{ (at 100\% power), i.e. } \rho_1 = -14.307 \text{ mk} \\
 k_1 &= 0.985848 \text{ (at 50\% power), i.e. } \rho_1 = -14.356 \text{ mk}
 \end{aligned}$$

Zone Controllers 35.5% full

$$\begin{aligned}
 k_0 &= 1.0 \\
 k_1 &= 0.986156 \text{ (at 100\% power), i.e. } \rho_1 = -14.039 \text{ mk}
 \end{aligned}$$

* PTB-20

TABLE VIMaterials used for generation of the modes

<u>MAT*</u>	<u>Type of Material</u>
1	Artificial
2	Reflector
3	1/2 Reflector + 1/2 Core
4	3/4 Reflector + 1/4 Core
5	Core
6	Core + $\Delta\Sigma a$ (C.B.)
7	Core + 1/2 $\Delta\Sigma a$ (C.B.)
8	Core + $\Delta\Sigma a$ (O.B.)
9	Core + 1/2 $\Delta\Sigma a$ (O.B.)

TABLE VIIMaterials used in XIPOLML

<u>MAT*</u>	<u>Type of Material</u>
1	Artificial
2	Reflector
3	1/2 Reflector + 1/2 Core
4	3/4 Reflector + 1/4 Core
5	Core

* See Appendices.

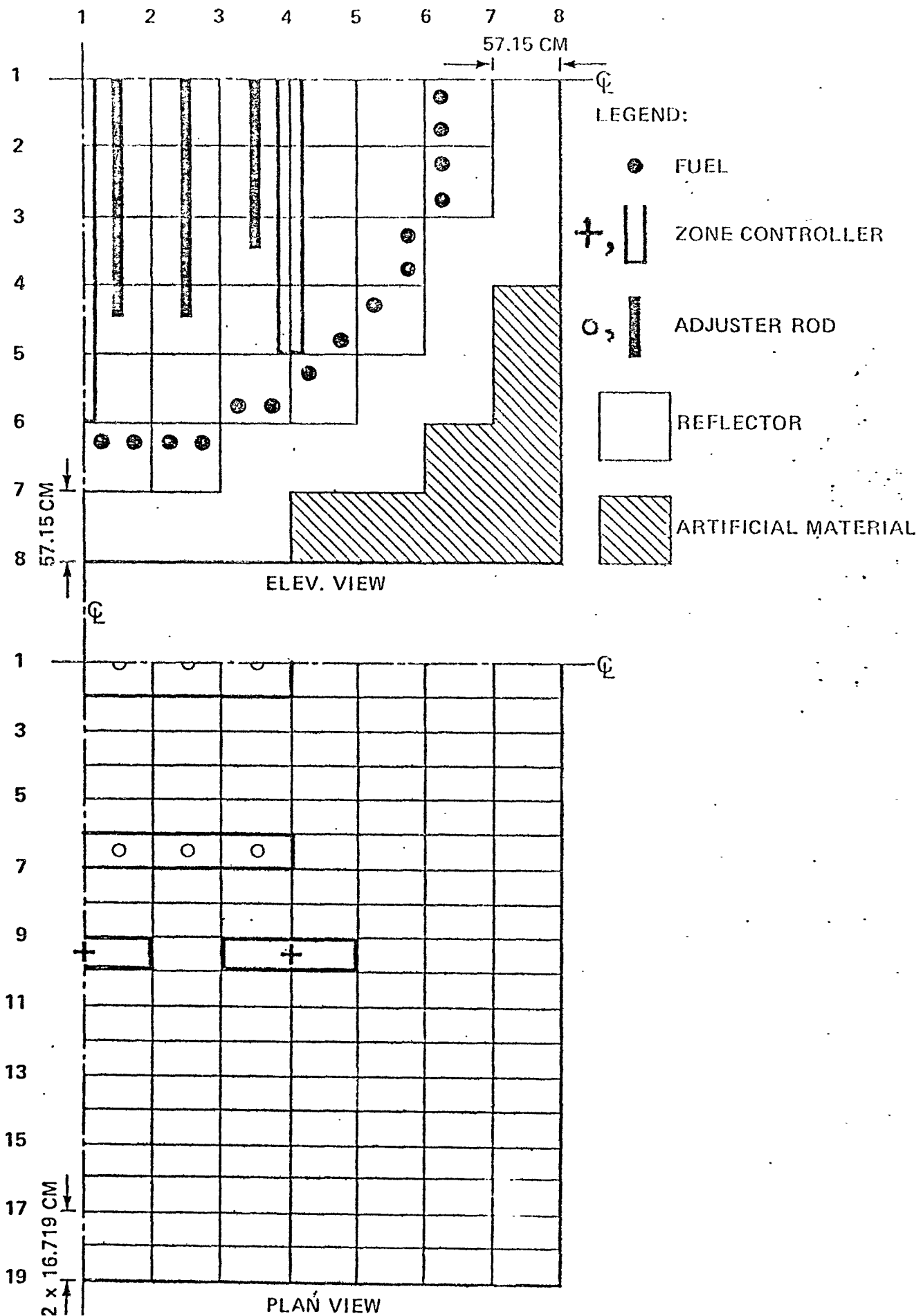
TABLE VIII

Threshold Power, Period and Physical Parameters for
100% and 50% of full power.

DATA	Distributions are created at 100% of Full Power conditions		Distributions are created at 50% of full power conditions. Zones almost empty.
	Zones almost empty	Zones at 35.5%	
Subcriticality (mk)	14.307	14.039	14.356
Ω	3.43×10^{-2}	3.37×10^{-2}	3.50×10^{-2}
η	5.62	5.69	5.54
Threshold Power (%)	39.9	38.1	42
Period (hrs.)	26.1	26.02	25.93

FIGURES

FIG.1 OCTANT CORE MODEL



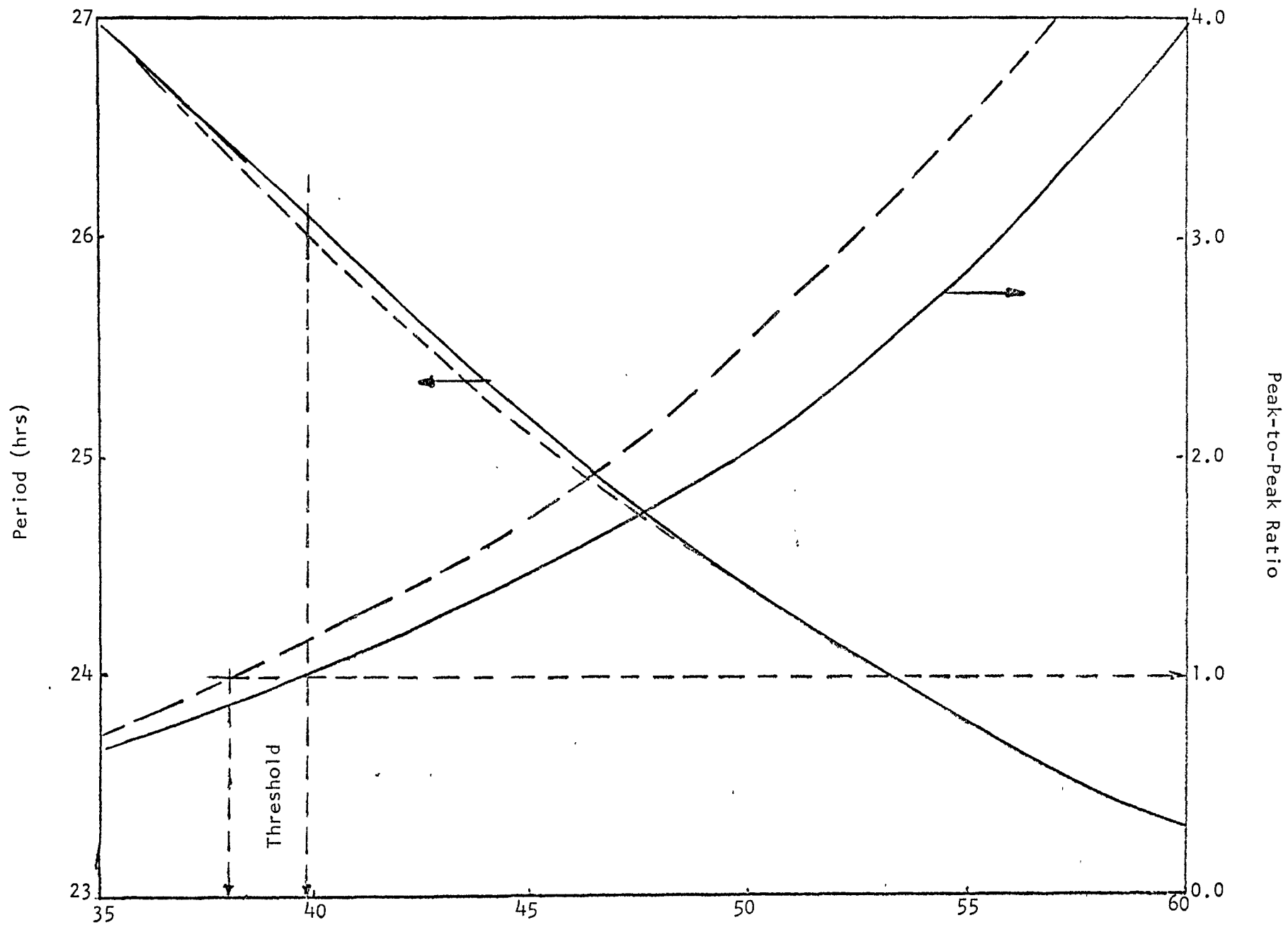


Figure 2 Side-to-Side Mode

Full Power (%)
 — Zones < 2%, $\rho = -14.307$ mk
 - - - Zones 35.5% full, $\rho = -14.039$ mk

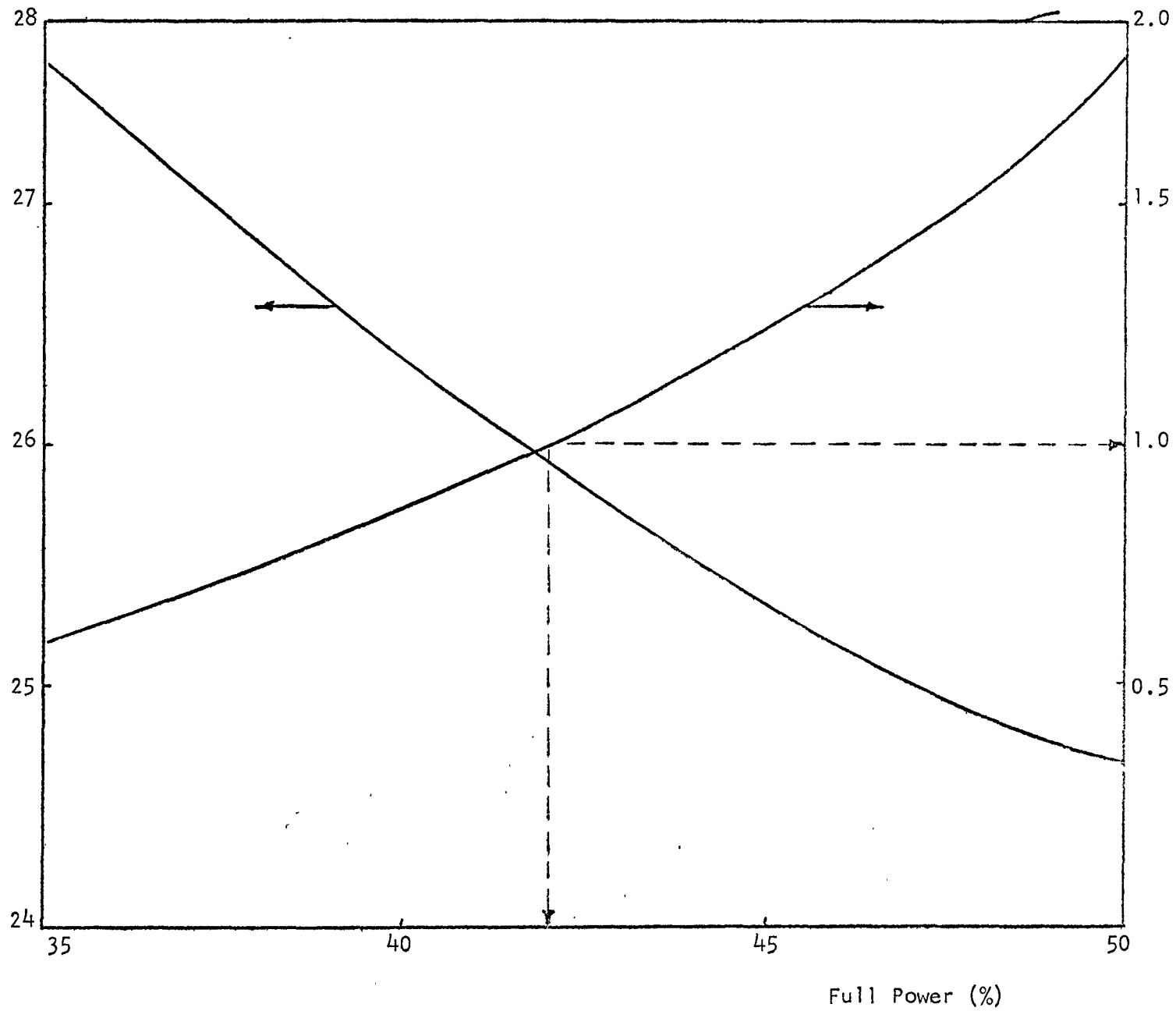


Figure 3 Side-to-Side Mode
 ($\phi = -14.356$ mk)

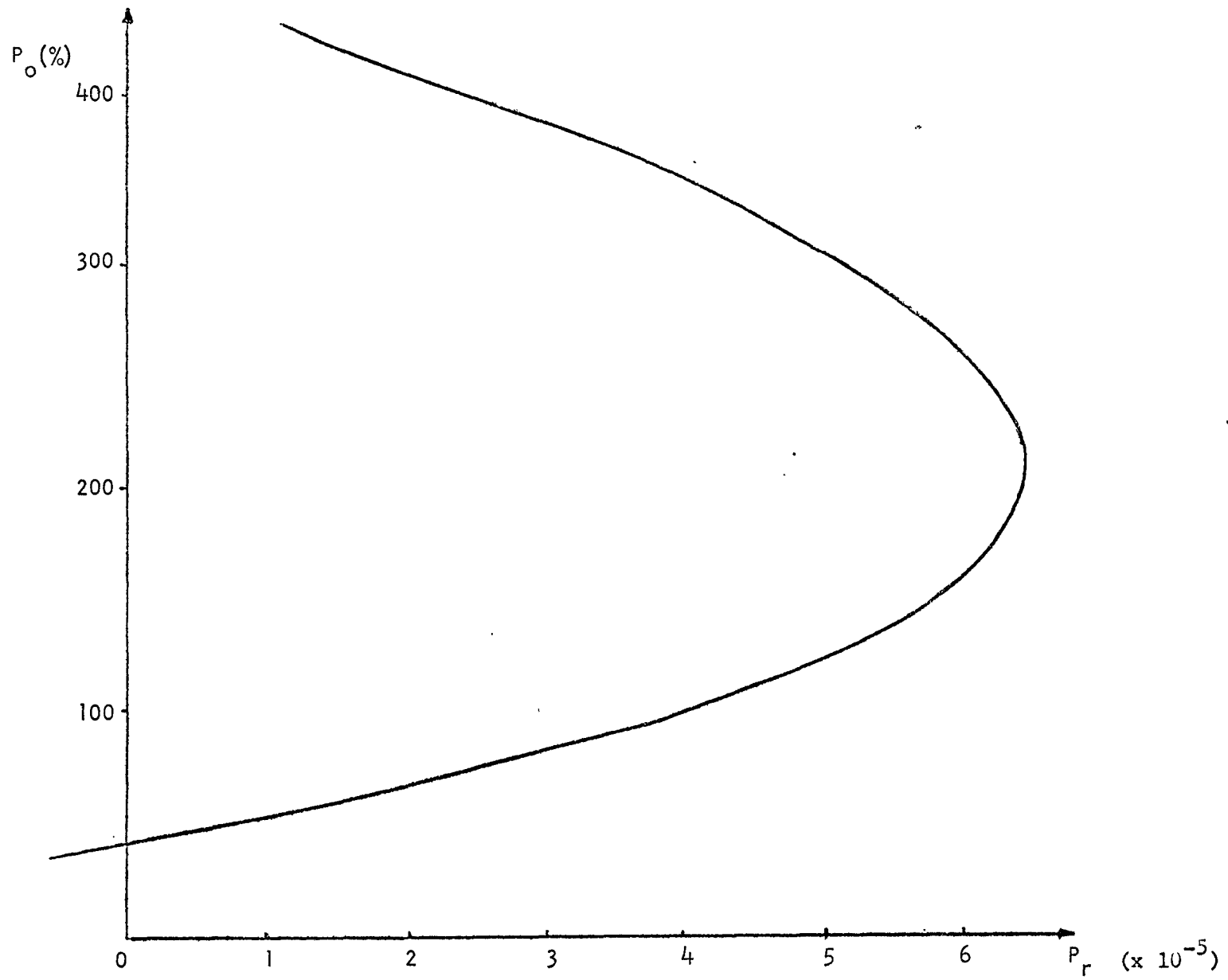


Figure 4 Power Level (%) vs the Real Part P_r

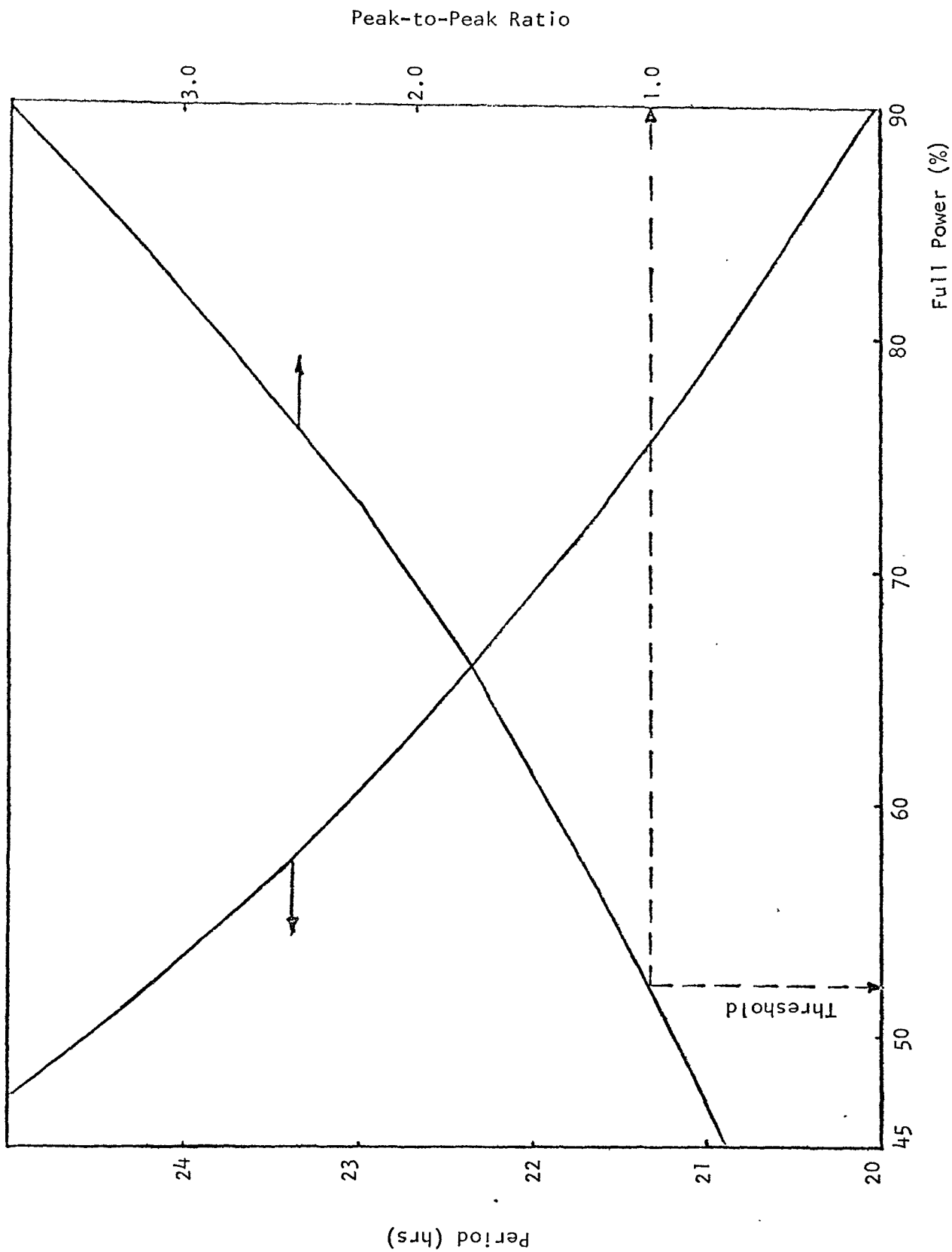


Figure 5 Side-to-Side Mode ($\omega = -16.24$ mk)

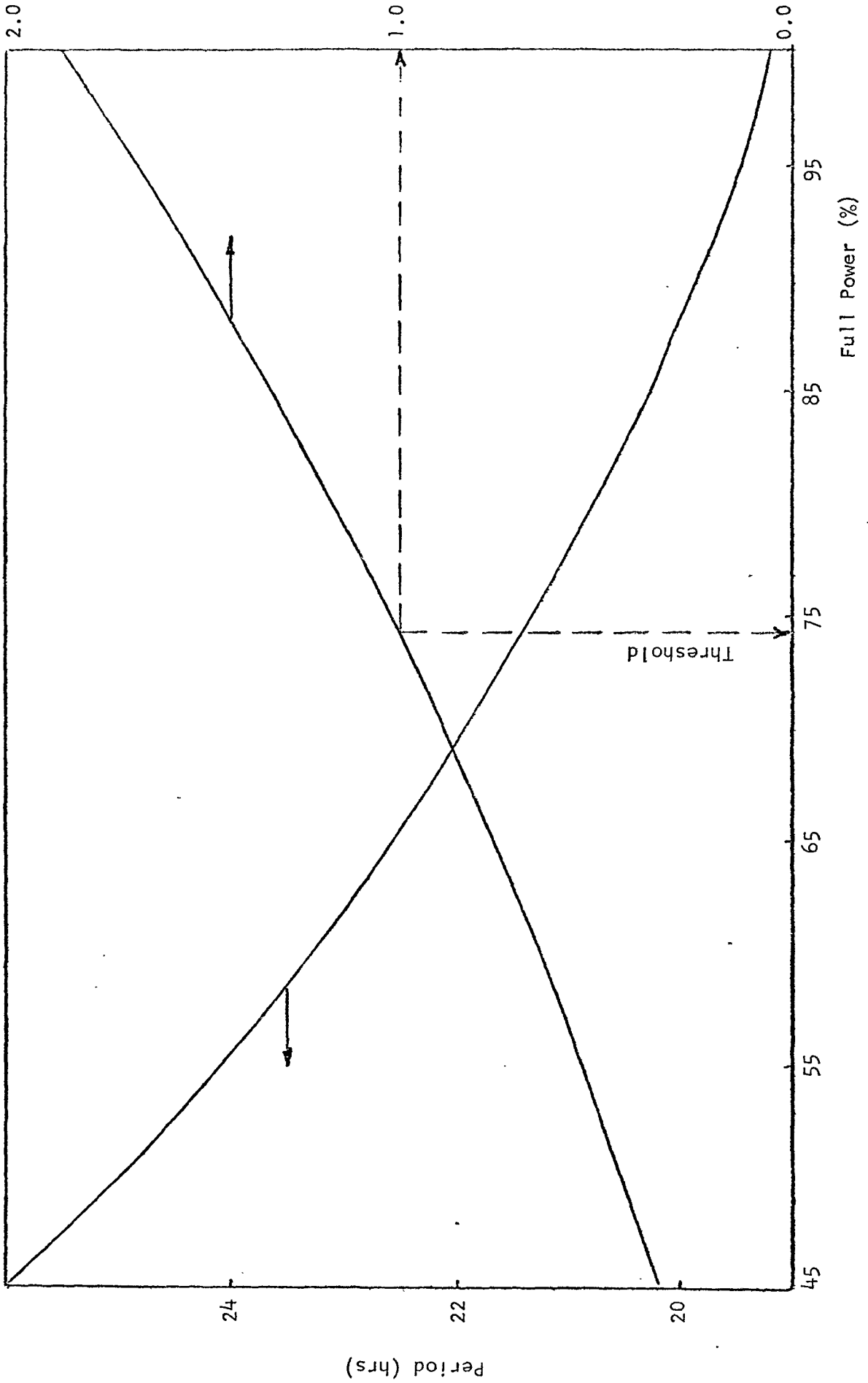


Figure 6 Side-to-Side Mode
($\rho = 18.0$ mk)

APPENDIX 1

XIPO1ML USER'S GUIDE

APPENDIX-1XIPO1ML USER'S GUIDE1. XIPO1ML PROGRAM

XIPO1ML Program consists of:

(1) Main Program

-- Handles the calculation of threshold power, and period of oscillation.

(2) Three Subroutines

- (a) HEAD - prints heading,
- (b) STDIZE - standardizes all input distributions, and
- (c) PRINTS - prints all input distributions.

2. DESCRIPTION OF TERMS

<u>FUND(I,J,K)</u>	The fundamental (thermal) flux (ϕ_o)
<u>XE(I,J,K)</u>	The xenon distribution (X_o)
<u>FAZ1(I,J,K)</u>	The fast first harmonic (Ψ_1)
<u>TAZ1(I,J,K)</u>	The thermal first harmonic (Ψ_2)
<u>FADJ1(I,J,K)</u>	The fast adjoint first harmonic (Ψ_1^*)
<u>TADJ1(I,J,K)</u>	The thermal adjoint first harmonic (Ψ_2^*)
<u>SF2(I)</u>	The thermal production term ($\nu\Sigma_{f,2}$)
<u>SR(I)</u>	The removal term (Σ_R)
<u>ALFA(I)</u>	The power coefficient which is associated with the fission cross section for a decrease in power from 100% to zero, and it is defined as in SORGHUM by the equation:

$$\nu\Sigma_{f,2}(\phi) = \nu\Sigma_{f,2}(\phi_o) \left(1 + \frac{\alpha_f(\phi - \phi_o)}{\phi_o} \right)$$

Where: α_f : flux (power) coefficient

ϕ_o : reference flux distribution

NMAT Maximum number of materials used in the model

NRX,NRY,NRZ The number of coordinates in the three dimensions (x,y,z)

NMAP 0 - - - No input distributions printed
 1 - - - ϕ_0 , printed
 >1 - - - $\phi_0 + \psi_2 + \psi_2^*$, printed

DX,DY,DZ The cell dimensions in the model used (cm)

XNU Neutrons born per fission

SIGXE The microscopic xenon thermal absorption cross section (cm²)

ZLAMI,ZLAMX The iodine and xenon decay constants (sec⁻¹)

GAMI,GAMX Fractional yield of iodine (I¹³⁵) and xenon (Xe¹³⁵) per fission

CKO,CK1 The fundamental (k_0) and first harmonic mode (k_1)
 criticality factors

FIN Input flux distribution level, in %

FNT Initial flux level in %, at which the threshold calculations
 start

FINCR Flux variation in %, for threshold calculations.
 (+ve):decrements
 (-ve):increments

NF Total number of flux steps for threshold calculations

3. Input Preparation

The input required for XIPOLML is described below. The input "data cards" must be in the order indicated below. The formats are given in parentheses immediately following the card description.

Card 1: Title Card (18A4)

Columns 1-72 TITLE - The information punched on this card is printed at the top of each page of output.

Card 2: Problem Parameters Card (5I5)

Columns 1-5 NMAP
 Columns 6-10 NRX
 Columns 11-15 NRY
 Columns 16-20 NRZ
 Columns 21-25 NMAP

Card 3: Threshold Calculations Card (I10,3F10.4)

Columns 1-5 NF
 Columns 6-10 FINCR
 Columns 11-15 FIN
 Columns 16-20 FNT

Card 4: Cell Dimensions Card (3F10.3)

Columns 1-10 DX
 Columns 11-20 DY
 Columns 21-30 DZ

Card 5: Xenon Parameters Card (6E10.3)

Columns 1-10 XNU
 Columns 11-20 SIGXE
 Columns 21-30 ZLAMI
 Columns 31-40 ZLAMX
 Columns 41-50 GAMI
 Columns 51-60 GAMX

Card 6: Mode Criticality Parameters (2F10.6)

Columns 1-10 CKO
 Columns 11-20 CK1

Card 7: Remarks Card(s) (18A4)

Columns 1-72 SUBS - These remarks will be printed at the beginning of the output. As many cards of remarks as may be desired may be used. Column 1 of each card is a carriage control symbol and should be left blank. The last remark card must have columns 1-4 inclusive blank, and no other remark card may have these four columns blank.

Card 8: Material Locations (7I5)

These cards give the initial and final coordinate numbers in each dimension for each material number. The overlay method is used, that is if the same volume is specified by two or more cards, the material number assigned by the last card read is used. The final coordinate numbers must exceed the initial coordinate numbers.

Columns 1-5	J1	The initial x-coordinate number
Columns 6-10	J2	The final x-coordinate number
Columns 11-15	J3	The initial y-coordinate number
Columns 16-20	J4	The final y-coordinate number
Columns 21-25	J5	The initial z-coordinate number
Columns 26-30	J6	The final z-coordinate number
Columns 31-35	J7	The number of the material which will occupy the volume bounded by the above coordinates. The maximum value of this number is NMAT.

The last of these cards must be followed by a blank card.

Card 9: Material Properties (3F10.3)

There are NMAT such cards in order of material number. The cross sections are macroscopic in units of cm^{-1} .

Columns 1-10 SF2
Columns 11-20 SR
Columns 21-30 ALFS

Flux Distributions (Unformatted) FUND, XE, FAZ1, TAZ1, FADJ1, TADJ1

The fundamental, the first harmonic and its adjoint, all generated with SORGHUM are read in on tape, in the following manner:

Fundamental on: unit TAPE3
First harmonic on: unit TAPE4
Adjoint First harmonic: unit TAPE5

4. Standard Coding Changes

All common cards must be exactly the same for both the main program and all the subroutines. Therefore all common cards within the program must be dimensioned properly, i.e.

FUND, XE, FAZ1, TAZ1, FADJ1, TADJ1, MAT, ARRAY must be dimensioned at least (NRX-1) by (NRY-1) by (NRZ-1)

APPENDIX II

XIPO1ML PROGRAM LISTING

```

PROGRAM XTPO1ML (INPUT,OUTPUT,TAPE10=INPUT,TAPE9=OUTPUT,
1 TAPE3,TAPE4,TAPE5)
COMMON FUND(8,8,18),XE(8,8,18),FAZ1(8,8,18),TAZ1(8,8,18),
1 FADJ1(8,8,18),TADJ1(8,8,18),MAT(8,8,18),SF2(50),SR(50),
2 ALFA(50),AMAX(3),NSCALP(3),ASCALP(3),ARRAY(8,8,18),
3 ITAZX,ITAZY,ITAZZ,IFUNDX,IFUNDY,IFUNDZ,ITADJX,ITADJY,ITADJZ
DIMENSION TITLE(18),SUBS(18)
DATA BLANK/4H /
C READ INPUT CHARACTERISTICS.
READ(10,99) TITLE
READ(10,15) NMAT,NRX,NRY,NRZ,NMAP
READ(10,98) NF,FINCR,FIN,FNT
READ(10,25) DX,DY,DZ
READ(10,30) XNU,SIGXE,ZLAMI,ZLAMX,GAMI,GAMX
READ(10,35) CKU,CKI
NPAGE=0
CALL HEAD(TITLE,NPAGE)
700 READ(10,99) SUBS
C WRITE INPUT CHARACTERISTICS.
WRITE(9,99) SUBS
IF(SUBS(1).NE.BLANK) GO TO 700
WRITE(9,113)
WRITE(9,116)
WRITE(9,101)
WRITE(9,102) NMAT,NRX,NRY,NRZ,NMAP
WRITE(9,103)
WRITE(9,104) DX,DY,DZ
WRITE(9,105)
WRITE(9,106) XNU,SIGXE,ZLAMI,ZLAMX,GAMI,GAMX
WRITE(9,107)
WRITE(9,108) CKU,CKI
WRITE(9,109)
WRITE(9,110) NF,FINCR,FIN,FNT
C READ MATERIAL MAP
200 READ(10,40) J1,J2,J3,J4,J5,J6,J7
J2=J2-1
J4=J4-1
J6=J6-1
DO 100 I=J1,J2
DO 100 J=J3,J4
DO 100 K=J5,J6
100 MAT(I,J,K)=J7
IF(J1.NE.0) GO TO 200
C READ MATERIAL PROPERTIES
DO 220 I=1,NMAT
220 READ(10,45) SF2(I),SR(I),ALFA(I)
C WRITE MATERIAL PROPERTIES.
CALL HEAD(TITLE,NPAGE)
WRITE(9,96)
DO 260 I=1,NMAT
260 WRITE(9,97) I,SF2(I),SR(I),ALFA(I)
DIFF=FIN-FNT
NRX=NRX-1
NRY=NRY-1
NRZ=NRZ-1
C READ THE DISTRIBUTIONS FROM TAPES.
READ(3) GARBAGE
READ(3) (((FUND(I,J,K),I=1,NRX),J=1,NRY),K=1,NRZ)

```

```

READ(3) GARRAGE
READ(3) (((XE(I,J,K),I=1,NRX),J=1,NRY),K=1,NRZ)
READ(4) (((FAZ1(I,J,K),I=1,NRX),J=1,NRY),K=1,NRZ)
READ(4) (((TAZ1(I,J,K),I=1,NRX),J=1,NRY),K=1,NRZ)
READ(5) (((FADJ1(I,J,K),I=1,NRX),J=1,NRY),K=1,NRZ)
READ(5) (((TADJ1(I,J,K),I=1,NRX),J=1,NRY),K=1,NRZ)
C
WRITE MATERIAL MAP
DO 290 K=1,NRZ
CALL HEAD(TITLE,NPAGE)
WRITE(9,90) K
DO 300 J=1,NRY
WRITE(9,95) (MAT(I,J,K),I=1,NRX)
300 WRITE(9,112)
290 CONTINUE
CALL STDIZE(NRX,NRY,NRZ)
IF(NMAP,LT,1) GO TO 800
M=1
DO 331 K=1,NRZ
DO 331 J=1,NRY
DO 331 I=1,NRX
331 ARRAY(I,J,K) = FUND(I,J,K)
CALL PRINTS(M,NRZ,NRY,NRX,TITLE,NPAGE)
IF(NMAP,LE,1) GO TO 800
M=2
DO 332 K=1,NRZ
DO 332 J=1,NRY
DO 332 I=1,NRX
332 ARRAY(I,J,K) = TAZ1(I,J,K)
CALL PRINTS(M,NRZ,NRY,NRX,TITLE,NPAGE)
M=3
DO 333 K=1,NRZ
DO 333 J=1,NRY
DO 333 I=1,NRX
333 ARRAY(I,J,K) = TADJ1(I,J,K)
CALL PRINTS(M,NRZ,NRY,NRX,TITLE,NPAGE)
800 CONTINUE
DO 718 J=1,NRY
DO 718 I=1,NRX
DO 718 K=1,NRZ
FUND(I,J,K) = FUND(I,J,K)*ASCALP(1)
TAZ1(I,J,K) = TAZ1(I,J,K)*ASCALP(2)
TADJ1(I,J,K) = TADJ1(I,J,K)*ASCALP(3)
718 CONTINUE
CALL HEAD(TITLE,NPAGE)
C
CALCULATION OF THE NORMALIZATION CONSTANTS
C
CALCULATION OF THE EFFECTIVE FLUX
SUMQ=SUMP=SUMH=SUMB=SUMA=0,0
VOL=DX*DY*DZ
DO 230 I=1,NRX
DO 230 J=1,NRY
DO 230 K=1,NRZ
IF(SF2(MAT(I,J,K)),EQ,0,0)GO TO 250
SUMP=SUMP+FUND(I,J,K)**3
SUMQ=SUMQ+FUND(I,J,K)**2
250 CONTINUE
SUMA=SUMA+FADJ1(I,J,K)*SF2(MAT(I,J,K))*TAZ1(I,J,K)
SUMR=SUMR+TADJ1(I,J,K)*SR(MAT(I,J,K))*FAZ1(I,J,K)
SUMH=SUMH+TADJ1(I,J,K)*XE(I,J,K)*TAZ1(I,J,K)

```

```

SUMA=SUMA*VOL
SUMB=SUMB*VOL*CK1
WRITE(9,114)
WRITE(9,50) SUMA,SUMB
WRITE(9,115)
WRITE(9,60) SUMP,SUMQ
EFFL=SUMP/SUMQ
WRITE(9,65) EFFL
C CALCULATION OF THRESHOLD
CALL HEAD(TITLE,NPAGE)
DO 400 M=1,NF
C FLUX-REDUCTION PARAMETER,
C=FNT-(M-1)*FINCR
WRITE(9,111) C
SUMG=SUMD=SUMF=0.0
IF(M.EQ.1.AND.DIFF.EQ.0.0) GO TO 500
SUMH=0.0
500 CONTINUE
DO 240 I=1,NRX
DO 240 J=1,NRY
DO 240 K=1,NRZ
SUMD=SUMD+TADJ1(I,J,K)*SF2(MAT(I,J,K))*TAZ1(I,J,K)/XNU
SUME=SUME+TADJ1(I,J,K)*SF2(MAT(I,J,K))*TAZ1(I,J,K)*FUND(I,J,K)*C
1(XNU*FIN)
SUMG=SUMG+TADJ1(I,J,K)*SF2(MAT(I,J,K))*TAZ1(I,J,K)*1.000000000*C
1*ALFA(MAT(I,J,K))/(XNU*1.00*FIN)
IF(M.EQ.1.AND.DIFF.EQ.0.0) GO TO 240
SUMH=SUMH+(GAMX+GAMI)*SF2(MAT(I,J,K))*(C*FUND(I,J,K)/(XNU*FIN))
1*TADJ1(I,J,K)*TAZ1(I,J,K)/(ZLAMX+SIGXE*(C*FUND(I,J,K)/FIN))
240 CONTINUE
SUMD=SUMD*VOL
SUME=SUME*VOL
SUMG=SUMG*VOL
IF(M.EQ.1.AND.DIFF.EQ.0.0) GO TO 600
SUMH=SUMH*VOL
600 WRITE(9,55) SUMD,SUME,SUMG,SUMH
C CALCULATION OF ETA-BETA-OMEGA.
ETA=SIGXE*SUME/(ZLAMX*SUMD)
OMEGA=((1./CK1-1./CK0)*SUMA*1.00-SUMG)/SUMD
BETA=(GAMI+GAMX)*SUME/(ZLAMX*SUMH)-1.0
WRITE(9,70) ETA,BETA,OMEGA
C CALCULATION OF THE PEAK-TO-PEAK-RATIO AND THE THE PERIOD
C PR=REAL PART OF OMEGA.
COL=COEFF C
C FR=IMAGINARY PART OF OMEGA.
PR=(1.+ZLAMI/ZLAMX+ETA-(ETA/OMEGA)*((GAMI+GAMX)*ETA/(1.+BETA)-
1GAMX))*ZLAMX/2.
COL=ZLAMI*ZLAMX*((1.+ETA)+(ETA*(GAMI+GAMX)/OMEGA)*(1.-ETA/
1(1.+BETA)))
FR=SQRT(ABS(COL-PR*PR))
WRITE(9,75) PR,COL,FR
PERIOD=3.14159/(FR*1800)
GR=FXP(-PR*PERIOD*3600,0)
WRITE(9,80) GR,PERIOD
15 FORMAT(5I5)
25 FORMAT(3F10.3)
30 FORMAT(6F10.3)

```

```

35 FORMAT(2F10,6)
40 FORMAT(7I5)
45 FORMAT(3E10,3)
50 FORMAT(1X,*SUMA=*,E12,6,5X,*SUMB=*,E12,6///)
55 FORMAT(1X,*SUMD=*,E12,4,5X,*SUMF=*,E12,4,5X,*SUMG=*,E12,4,5X,
  1*SUMH=*,E12,4///)
60 FORMAT(1X,*SUMP=*,E12,6,5X,*SUMQ=*,E12,6///)
65 FORMAT(1X,*EFFL=*,1PE12,6///)
70 FORMAT(1X,*ETA=*,0PF12,7,5X,*BETA=*,0PF12,7,5X,*OMEGA=*,1PE16,7//)
75 FORMAT(1X,*PR=*,1PE16,7,5X,*COL=*,1PE16,7,5X,*FR=*,1PE16,7///)
80 FORMAT(1X,*PEAK=10-PEAK RATIO=*,F10,4,5X,*PERIOD=*,F10,3///)
90 FORMAT(6X,*MATERIAL MAP AT LEVEL*,4X,*Z=*,I2,/)
95 FORMAT(8X,35I3)
96 FORMAT(* MATERIAL CONSTANTS*/11X,*PROD(2)          REMOVAL          PI
  1D COEFF*//)
97 FORMAT(18,1P3F14,4)
98 FORMAT(110,3F10,4)
99 FORMAT(18A4)
101 FORMAT(10X,*NMAT NRX NRY NRZ NMAP*//)
102 FORMAT(6X,5I6//)
103 FORMAT(* CELL DIMENSIONS*/11X,*DX          DY          DZ*//)
104 FORMAT(7X,3F10,3//)
105 FORMAT(* XENON PARAMETERS*/11X,*XNU          SIGXE          ZLAMI
  1 ZLAMX          GAMI          GAMX*//)
106 FORMAT(7X,1P6E13,3//)
107 FORMAT(* MULTIPLICATION CONSTANTS*/11X,*KEFF(FUND)          KEFF(AZI
  1)*//)
108 FORMAT(4X,2F15,6//)
109 FORMAT(* CHANGE IN POWER LEVEL*/12X,*NF          INCREM          INPUT
  1 INITIAL*//)
110 FORMAT(1X,I12,3F12,4)
111 FORMAT(2X,*CALCULATION AT POWER LEVEL =*,F7,2,///)
112 FORMAT(1H )
113 FORMAT(1H0)
114 FORMAT(1X,*NORMALIZATION INTEGRALS*//)
115 FORMAT(1X,*EFFECTIVE FLUX CALCULATIONS*//)
116 FORMAT(* PROBLEM PARAMETERS*)
  CALL HEAD(TITLE,NPAGE)
400 CONTINUE
  STOP
  END
  SUBROUTINE HEAD(T,NP)
  DIMENSION T(18)
  IF (NP) 10,10,20
  10 CALL DATF(DAT)
  TIMIN=SECOND(A)
  20 TN=SECOND(A)-TIMIN
  NP=NP+1
  WRITE (9,1000) T,NP,DAT,TN
1000 FORMAT (1H1,18A4,9H          PAGE,I4,5X,A10,6H          TIME,F6,2,4H SEC//)
  RETURN
  END
  SUBROUTINE PRINTS(L,NRZS,NRYS,NRXS,XTITLE,NPAG)
  COMMON FUND(8,8,18),XE(8,8,18),FAZI(8,8,18),TAZI(8,8,18),
  1 FADJ1(8,8,18),TADJ1(8,8,18),MAT(8,8,18),SF2(50),SR(50),
  2 ALFA(50),AMAX(3),NSCALP(3),ASCALP(3),ARRAY(8,8,18),
  3 ITAZX,ITAZY,ITAZZ,IFUNDX,IFUNDY,IFUNDZ,ITADJX,ITADJY,ITA
  INDICI = 0

```

```

INDIC2 = 0
COUNT = 0
IF(NRYS,LF,28,AND,NRX,LE,17) INDIC1 = 1
DO 20 K=1,NRZS
IF(INDIC1,EQ,1,AND,COUNT,NE,0,0) GO TO 77
CALL HEAD(XTITLE,NPAG)
77 IF(L,FO,1) WRITE(9,10) K,NSCALP(L)
IF(L,FO,2) WRITE(9,11) K,NSCALP(L)
IF(L,FO,3) WRITE(9,12) K,NSCALP(L)
COUNT=COUNT + 1
NX1= 17
NC1= 1
616 NI = MIN0(NX1,NRXS)
IF(INDIC2,EQ,1) WRITE(9,741)(I,I=NC1,NI)
IF(INDIC2,NE,1) WRITE(9,740)(I,I=NC1,NI)
WRITE(9,22)
JVI=0
DO 614 J=1,NRYS
JVI = JVI + 1
IF(INDIC2,NE,1) GO TO 618
WRITE(9,719) JVI,(ARRAY(I,J,K),I=NC1,NI)
GO TO 614
618 WRITE(9,718) JVI,(ARRAY(I,J,K),I=NC1,NI)
614 CONTINUE
617 IF(NRYS=NX1) 619,619,615
615 WRITE(9,718)
INDIC2=1
NC1 = NC1 + 17
NX1 = NX1 + 17
GO TO 616
619 CONTINUE
INDIC2 = 0
WRITE(9,52)
IF(COUNT,FO,2,0) COUNT = 0,0
20 CONTINUE
IF(L,FO,1)WRITE(9,788)AMAX(1),IFUNDZ,IFUNDY,IFUNDX
IF(L,FO,2)WRITE(9,788)AMAX(2),ITAZZ,ITAZY,ITAZX
IF(L,FO,3)WRITE(9,788)AMAX(3),ITADJZ,ITADJY,ITADJX
10 FORMAT(6X,*MAP OF FUNDAMENTAL FLUX AT LEVEL*,4X,*Z=*,I2,50X,*(1,0
1-*,I2,*)*,/)
11 FORMAT(6X,*MAP OF FIRST HARMONIC FLUX AT LEVEL*,4X,*Z=*,I2,50X,*(
1,0E-*,I2,*)*,/)
12 FORMAT(6X,*MAP OF ADJOINT FIRST HARMONIC FLUX AT LEVEL*,4X,*Z=*,I
1,50X,*(1,0E-*,I2,*)*,/)
741 FORMAT(11X,17I7,/)
740 FORMAT(3X,17I7,/)
22 FORMAT(1H )
719 FORMAT(13,10X,17F7,2)
718 FORMAT(13,2X,17F7,2)
52 FORMAT(1H0)
788 FORMAT(20X,*MAXIMUM FLUX VALUE =*,2X,1PF15,5 ,5X,*LOCATI
IN IS PLANE NO,*,2X,I2,2X,*ROW NO,*,2X,I2,2X,*COLUMN NO,*,2X,I2,/)
RETURN
END
SUBROUTINE STDIZE(NRXS,NRYS,NRZS)
COMMON FUND(8,8,18),XE(8,8,18),FAZI(8,8,18),IAZI(8,8,18),
1 FADJ1(8,8,18),TADJ1(8,8,18),MAT(8,8,18),SF2(50),SR(50),
2 ALFA(50),AMAX(3),NSCALP(3),ASCALP(3),ARRAY(8,8,18),

```



```
3      ITAZX,ITAZY,ITAZZ,IFUNDX,IFUNDY,IFUNDZ,ITADJX,ITADJY,ITADJZ
      AMAX(1) = FUND(I,1,1)
      AMAX(2) = TAZI(I,1,1)
      AMAX(3) = TADJ1(I,1,1)
      DO 631 J=1,NRYS
      DO 631 I=1,NRXS
      DO 631 K=1,NRZS
      IF(FUND(I,J,K).LE.AMAX(1))GO TO 632
      AMAX(1) = FUND(I,J,K)
      IFUNDX = I
      IFUNDY = J
      IFUNDZ = K
632 IF(TAZI(I,J,K).LE.AMAX(2))GO TO 633
      AMAX(2) = TAZI(I,J,K)
      ITAZX = I
      ITAZY = J
      ITAZZ = K
633 IF(TADJ1(I,J,K).LE.AMAX(3))GO TO 651
      AMAX(3) = TADJ1(I,J,K)
      ITADJX = I
      ITADJY = J
      ITADJZ = K
631 CONTINUE
      DO 650 I=1,3
      NSCALP(I) = INT(ALOG10(AMAX(I)))-2
650 ASCALP(I) = 10.0**(NSCALP(I))
      DO 652 J=1,NRYS
      DO 652 I=1,NRXS
      DO 652 K=1,NRZS
      FUND(I,J,K) = FUND(I,J,K)/ASCALP(1)
      TAZI(I,J,K) = TAZI(I,J,K)/ASCALP(2)
      TADJ1(I,J,K) = TADJ1(I,J,K)/ASCALP(3)
652 CONTINUE
      RETURN
      END
```